BNL 37707

CONF-850734--22

A THERMAL ABSORBER FOR HIGH POWER DENSITY PHOTON BEAMS

MAR 24 1986

S. Ulc and S. Sharma

Brookhaven National Laboratory, Upton, New York 11973, USA

BNL--37707

DE86 008012

ABSTRACT

The high power density of multipole wiggler radiation from the X-ray ring at the National Synchrotron Light Source at Brookhaven National Laboratory precludes the use of normal incidence water cooled masks and shutters due to high metal temperatures and resulting high stresses and/or deflections and the possibility of cooling water boiling. One way the power density can be reduced is by positioning the absorber surface at a small angle to the beam, a technique first developed by Lawrence Berkeley Laboratory. Finite element analyses results for temperatures, displacements and stresses are presented in this paper for a thermal absorber designed for ultra-high vacuum operation.

1. Introduction

The basic absorber is a continuous length of hollow core O.F. copper conductor which has been formed and machined into the required shape and positioned so as to intercept the photon beam at a small angle (see Fig. 1). Water connections are made outside the vacuum containment. The advantage of this approach is that fabrication is relatively simple, there are no water-vacuum joints and only two permanent atmosphere to vacuum seals (brazed joints) are required.

A two-dimensional finite element analysis is first carried out to obtain the temperature distribution across the absorber cross-section. The resulting thermal deflections and stresses are then obtained by two coupled structural analyses utilizing plane-strain formulation and beam finite elements. Numerical results for maximum deflections and stresses are compared to their corresponding design values.

2. Thermal Analysis

The normal incidence peak power density from the X-ray ring superconducting wiggler at 10m from the source is 3880 W/cm^2 with a nearly Gaussian distribution in the vertical plane[1]. Positioning the absorbing surface at 6° in the horizontal plane to the photon beam (Fig. 1) reduces the peak power density to 406 W/cm^2 (3880 W/cm^2 x sin 6°). The absorber cross-section itself is 5/8" x 1" with a 3/8" diameter water channel through the center. A velocity of 20 ft/sec was assumed in the water channel resulting in a 7 gal/min flow and a pressure drop of 3 psi per foot of absorber length. At a water inlet temperature of 25°C, a value of 2.1 $W/(°C\ cm^2)$ for the film coefficient for turbulent flow was determined by means of the expression[2]

$$h_f = \frac{V^{0.8}}{d_h^{0.2}} (0.118 + 0.0016T_b) \frac{W}{°C\ cm^2}$$

where V = water velocity, ft/sec.

d_H = water channel diameter, inches

T_b = bulk water temperature, °C

Using the absorber geometry, power input and cooling parameters, a 2-dimensional finite element solution was obtained for the temperature distribution within the absorber cross-section. Approximately 500 temperatures were determined yielding important maximum values such as copper temperature, water cooling channel wall temperature (to determine the possibility of boiling) and temperature drop across the film.

Fig. 2a shows the temperature distributions throughout the absorber cross-section when the photon beam is directly over the cooling channel and Fig. 2b shows them when the beam is near the edge of the absorber corresponding to a maximum shift of the beam centerline. These temperatures are based on a water inlet temperature of 25°C. There is a bulk water temperature rise in the absorber of

$$\Delta T\Big|_{bulk} = \frac{3.8 \times kW}{GPM} = \frac{3.8(7.8)}{7} = 4.2C°$$

The maximum cooling channel wall temperature is 66.4°C (62 + 4.2), low enough to preclude any possibility of boiling.

If the absorber is positioned at a small angle in the vertical plane it sees a peak power density at its center decreasing toward its ends as shown in Fig. 3a. It sees the beam across its entire width resulting in a maximum power/unit length of 343 W/cm (about 3 times that of the 6° horizontal absorber) at an angle of 2° to the beam. This is about the smallest angle that can be used due to thermal deflections, fabrication tolerances and alignment requirements. Thermal analysis results (Fig. 3b) indicate a maximum copper temperature of 112°C and a maximum water channel temperature of 97°C which is close to the atmospheric boiling temperature of 100°C. Boiling should be avoided in order not to generate steam voids and resulting hot spots. By increasing the exit pressure to 10 psig the saturation (boiling) temperature at 10 psig increases to 116°C. The inlet must necessarily be higher due to the pressure drop in the channel. The bulk water temperature rise is 1.3C°.

3. Stress Analysis

A finite element plane-strain stress analysis technique was used to determine the stress and strain distributions in the cross-sectional plane of the absorber. This technique assumes that the temperature, stresses and strains do not vary along the absorber's length and its ends are initially fixed (see Fig. 4). The absorber should not be fixed on its sides since that increases the degree of restraint which increases the stress level. Two sides and both ends fixed increases the stress by a factor of $1/(1-\nu)$ (ν is Poisson's ratio) = $1/(1-.33)$ = 1.5. All four sides and both ends fixed increases the stress by a factor of $1/(1-2\nu)$ or $1/(1-.67)$ = 3.

The temperature results as previously determined are used as inputs to the stress analysis program. The relations representing the equilibrium of each element and the conditions for continuity between the elements are solved directly. The normal stresses s_x and s_y and shear stress s_{xy} in the plane of the cross-section are computed for each element and the axial stress s_z is determined from the expression

$$s_z = \nu(s_x + s_y) - E\alpha T \text{ (for fixed ends)} \qquad [3]$$

where ν is Poisson's ratio

E is modulus of elasticity

α is thermal expansion coefficient

T is temperature change of element

By combining s_x, s_y and s_{xy} the in-plane principal stresses s_1 and s_2, (maximum and minimum normal stresses) are determined for each element by means of the expression

$$s_1, s_2 = \frac{s_x + s_y}{2} \pm \left(\left(\frac{s_x - s_y}{2} \right)^2 + s_{xy}^2 \right)^{1/2} \qquad [4]$$

The absolute values of principal stress differences $|s_1 - s_2|$, $|s_1 - s_z|$ and $|s_2 - s_z|$ are computed and the maximum of the three is compared to a design stress. Typically the axial stress s_z is largest compared to s_1 or s_2 and is at the point of maximum copper temperature (point A in Fig. 4). The advantage of fixing the ends is that for a constant thermal moment at each section, counteracting equal moments are developed at the ends resulting in no absorber displacement. The product of s_z and the area on which it acts ΔA_{ax} is the axial force on each element and when summed across all elements is the axial restraining force on the absorber. In addition, this elemental axial force when multiplied by its distance to each of the two neutral axes and summed over all elements results in the previously mentioned restraining moments acting on the ends of the absorber. The program determines the stresses when one end is fixed and the other is free by applying the fixed ended elemental forces and moments of opposite sign to the ends of the absorber. The resultant maximum stress values for an absorber with a free end are about 1/3 to 1/12 of the fixed ends values and do not occur at the point of maximum copper temperature but typically at the water channel wall on the side away from the photon beam (point B in Fig. 4). Table 1 summarizes these results. The resultant absorber displacements (deflections and slopes; 0.160" and 0.8° maximum) for the fixed/free condition are large. Due to the configuration of the absorber (the two loops at each end act as compliant structural members — see Fig. 1), one end constraint can be adjusted (the other end being fixed) by shifting the position of the support section near the loop to optimize the stress/displacement characteristics.

The upstream end is fixed because the slight beam incident angle increase near the fixed end due to thi thermal heating is less than if the downstream end was fixed. The angle increase should be minimized as it results in greater power density on the absorber.

4. Absorber Stress/Deflection Analysis

A finite element beam-frame stress analysis program w utilized to determine stresses and displacements of the actual absorber. This method requires inserting the axial force and moments, as determined from the fixed ends solution, into the frame at the location corresponding to the two ends of the power input section (see Fig. 5).

The applied axial force and moments re-distribute themselves throughout the frame depending on the geometry, elasticity and boundary conditions of each finite element beam with the resultant axial force, F_{ax}, moments M_x, M_y, and displacements (3 translation, 3 rotation) at each beam being determined. The resulting axial stress s_z is determined by the following expression which combines the axial and bending stresses:

$$s_z = \pm \frac{F_{ax}}{A_{ax}} \mp \frac{M_y}{I_y} x \pm \frac{M_x}{I_x} y$$

where at each section:

F_{ax} is the axial force

A_{ax} is the axial cross-section

M_y, M_x are the moments about orthogonal axes

I_y, I_x are the moments of inertia about orthogonal axes

x, y are the distances of the element from the respective neutral axes

This resulting value of s_z is now combined with s_1 and s_2 as previously determined from the plane-strain analysis to determine the actual principal stress differences as before and the maximum of these is compared to the allowable thermal stress. There are two basic types of thermal stresses. One type causes excessive distortions of the entire structure and the allowable stress is twice the annealed O.F. copper yield strength (2 times 8000 psi) [9]. The other produces no significant displacements and fatigue strength is used as a criteria for failure since thermal cycling will occur during normal operating procedures.

For a ten year life, a conservative value of 10^5 cycles (40 times a day x 250 days/yr) was assumed. A number of sources[5-8] were used to determine actual test failure levels of stress of annealed O.F. copper for various cycle times. A conservative value of stress failure level was used and a safety factor of 2 was applied to determine the design stress. At 10^5 cycles the design stress single amplitude is 7500 psi. The computed maximum principal stress difference was compared to the stress range (double amplitude) or 15,000 psi. This is the basic procedure followed by the ASME Pressure Vessel Code in designing pressure vessels for fatigue [9].

Fig. 6 shows the resultant values of moments, axial forces, stresses, and displacements for a typical absorber positioned in the horizontal plane and a beam splitter positioned in the vertical plane.

Work done at Brookhaven is supported by the Division of Materials Sciences, U.S. Dept. of Energy, under contract DE-AC02-76CH00016.

REFERENCES

1. Thomlinson, W., "X-Ray Power Distribution from Multipole Wiggler Magnets," April 1983, internal memorandum.
2. "Heat Transmission," McAdams, W.H. 1942.
3. "Elements of Thermal Stress Analysis," Burgreen, D., 1971.
4. "Strength of Materials," Singer, F.L. 1951.
5. "A Survey of Properties and Applications, OFHC Brand Copper," Amax Copper, Inc. 1270 Ave. of the Americas, NY, NY 10020.
6. "Stress-Strain Relationships in Low and Intermediate Cycle Fatigue," Blatherwick, A. and Mowbray, D., ASTM Proc. 64, 561-578 (1964).
7. "Experimental Support for Generalized Equation Predicting Low Cycle Fatigue," Tavernelli, J. and Coffin, L., ASME Jour. of Basic Engineering, Dec. 1962, 533.
8. "Standards Handbook," Alloy Data, Copper Development Association, Inc. 405 Lexington Avenue, NY, NY 10007.
9. ASME Boiler and Pressure Vessel Code, Section VIII, Division 2, 1982.

Figure Captions

Fig. 1 Conceptual Design: 6° Horizontal Absorber.

Fig. 2 Temperature Distribution: 6° Horizontal Absorber.
(a) zero beam shift. (b) maximum beam shift.

Fig. 3 2° Vertical Absorber. (a) geometry and power density distribution. (b) temperature distribution.

Fig. 4 Stress Components: Plane-Strain Analysis.

Fig. 5 Stress Analysis: Beam-Frame Model

Fig. 6 Resultant Stresses, Displacements and Reactions:
(a) 6° Horizontal Absorber. (b) 2° Vertical Absorber.

TABLE 1

STRESSES, DEFLECTIONS AND REACTIONS - FIXED/FREE END CONDITIONS

Horizontal Absorber @6°, 24" long

		Both Ends Fixed		One End Fixed, One End Free	
Photon Beam Pos. Figure No.		2a	2b	2a	2b
F_{ax}	lb	3430	3750	0	0
M_{y0}	lb-in	138	110	0	0
M_{x0}	lb-in	0	390	0	0
s_{max}	psi	15700	20000	5970	6600
$\delta_{y,max}$	inch	0	0	0	0.16
$\delta_{x,max}$	inch	0	0	0.13	0.10
$\theta_{y,max}$	deg	0	0	0.62	0.50
$\theta_{x,max}$	deg	0	0	0	0.80

Vertical Absorber (Splitter @2°), 24" long

		Both Ends Fixed	One End Fixed, One End Free
Photon Beam Pos. Figure No.		3b	3b
F_{ax}	lb	8590	0
M_{y0}	lb - in	322	0
M_{x0}	lb - in	0	0
s_{max}	psi	25500	2000
$\delta_{y,max}$	inch	0	0
$\delta_{x,max}$	inch	0	0.085
$\theta_{y,max}$	deg	0	0.22
$\theta_{x,max}$	deg	0	0

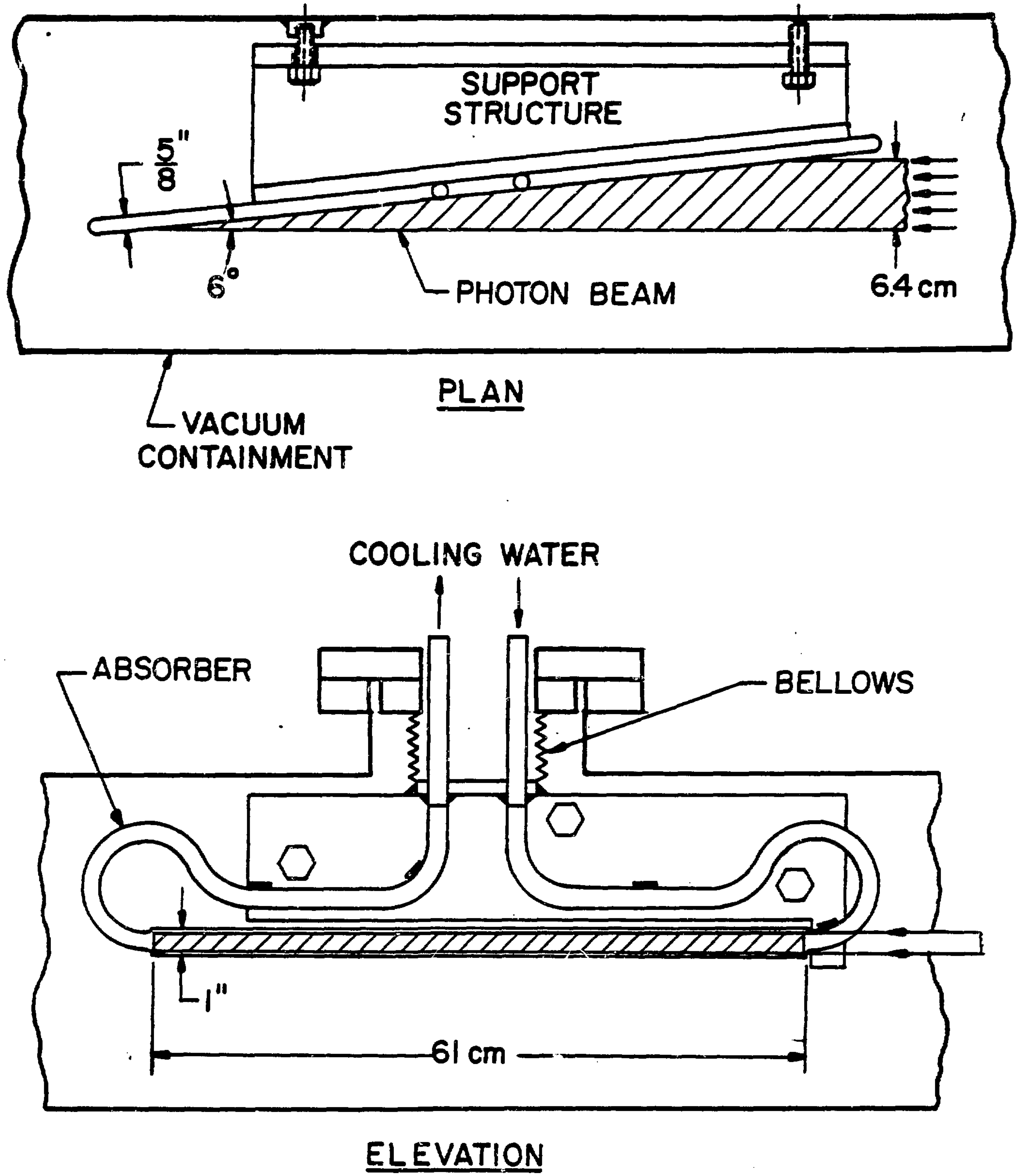
SUPPORT
STRUCTURE
5/8"
6°
PHOTON BEAM
6.4 cm
PLAN
VACUUM
CONTAINMENT
COOLING WATER
ABSORBER
BELLOWS
1"
61 cm
ELEVATION

FIG. 1

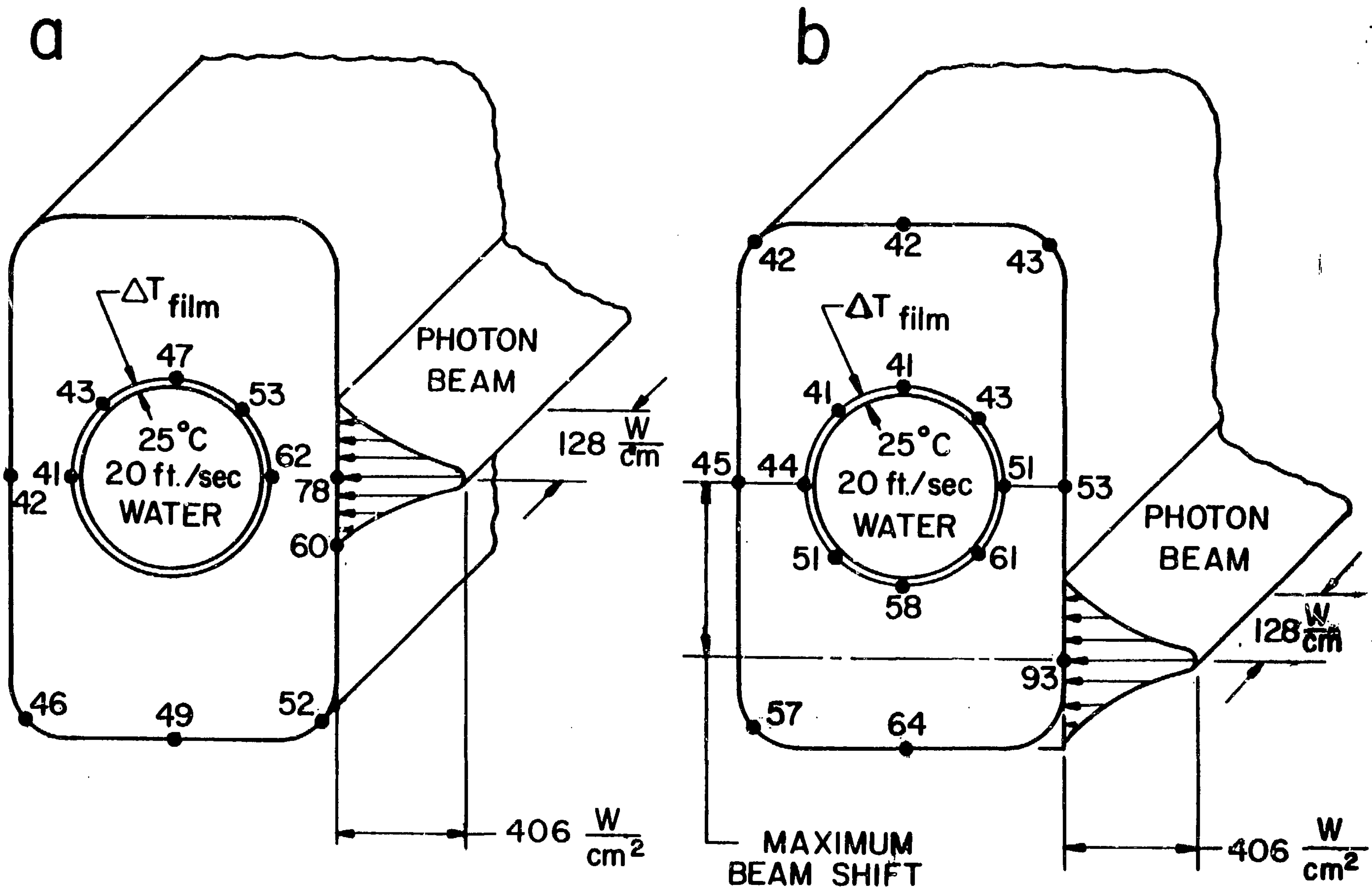

a
b
ΔT film
25°C
20 ft./sec
WATER
PHOTON
BEAM
128 W/cm
406 W/cm²
MAXIMUM
BEAM SHIFT
47
43
53
41
42
62
78
60
46
49
52
42
42
43
41
41
43
45
44
51
53
51
61
58
93
57
64

FIG. 2

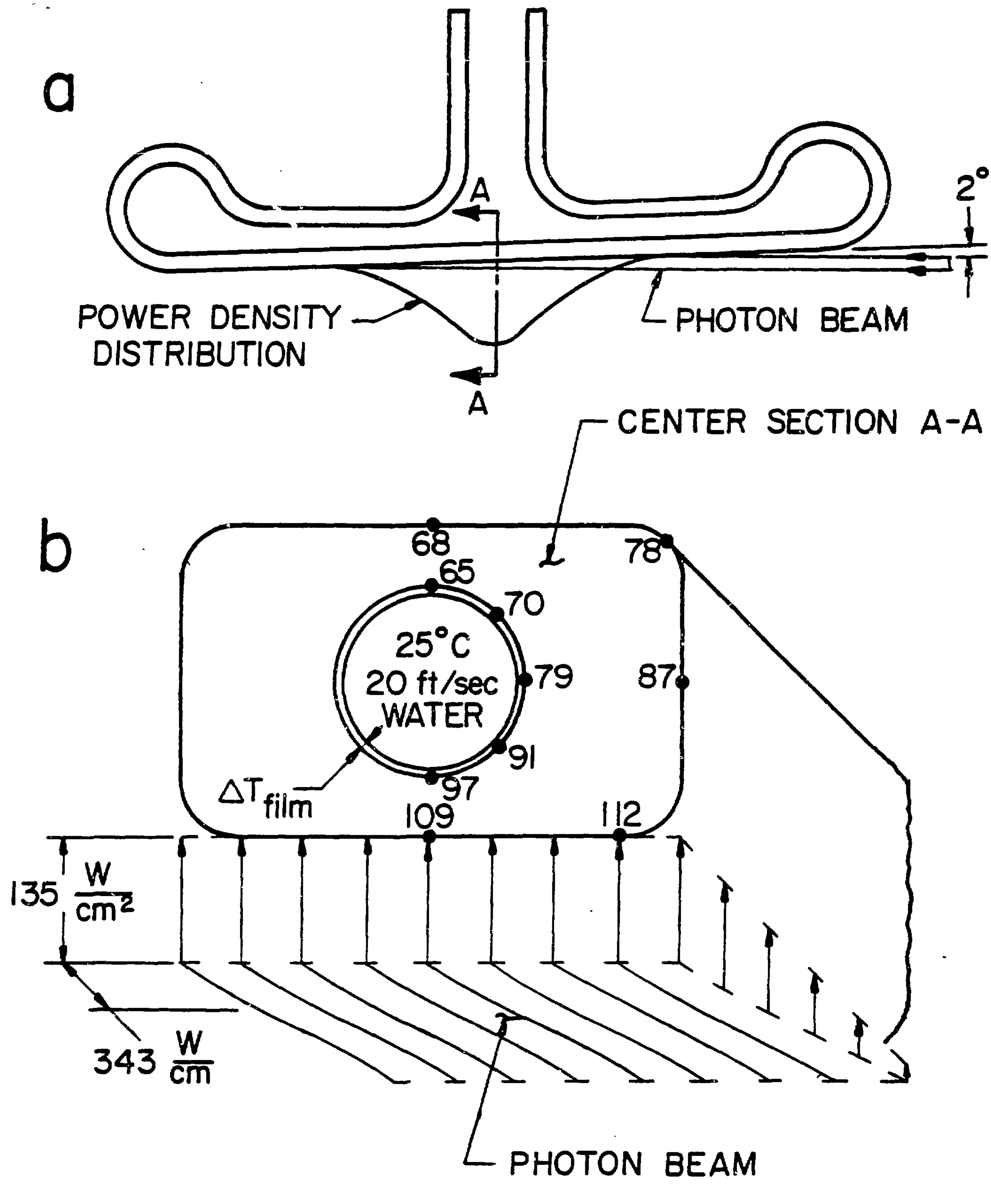
a
A
2°
POWER DENSITY DISTRIBUTION
PHOTON BEAM
A
CENTER SECTION A-A
b
68
65
78
70
25°C
20 ft/sec
WATER
79
87
91
97
ΔT film
109
112
135 W/cm²
343 W/cm
PHOTON BEAM

FIG. 3

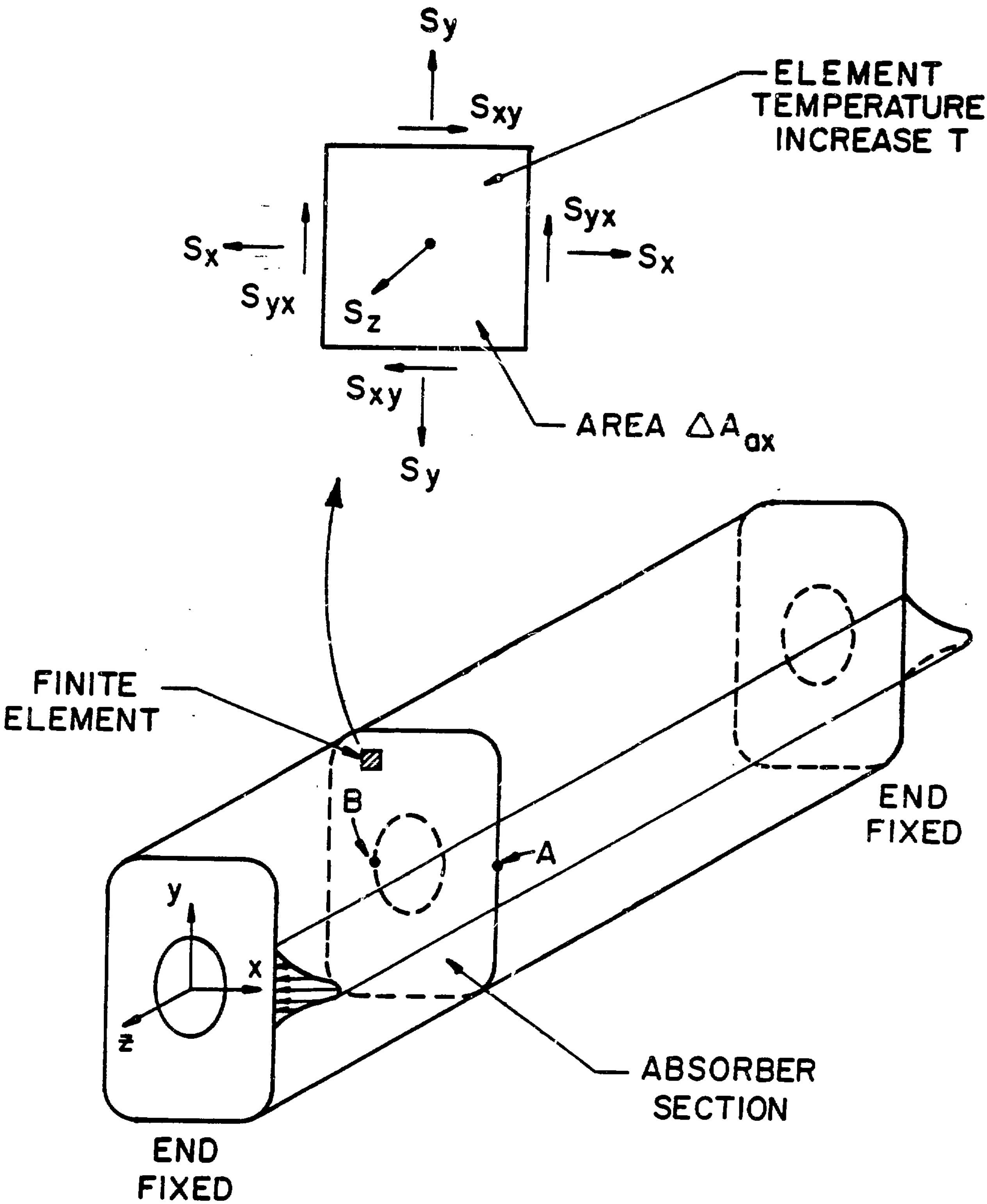

Sy
Sxy
ELEMENT TEMPERATURE INCREASE T
Syx
Sx
Sx
Syx
Sz
Sxy
AREA ΔAax
Sy
FINITE ELEMENT
B
A
y
x
z
END FIXED
ABSORBER SECTION
END FIXED

FIG. 4

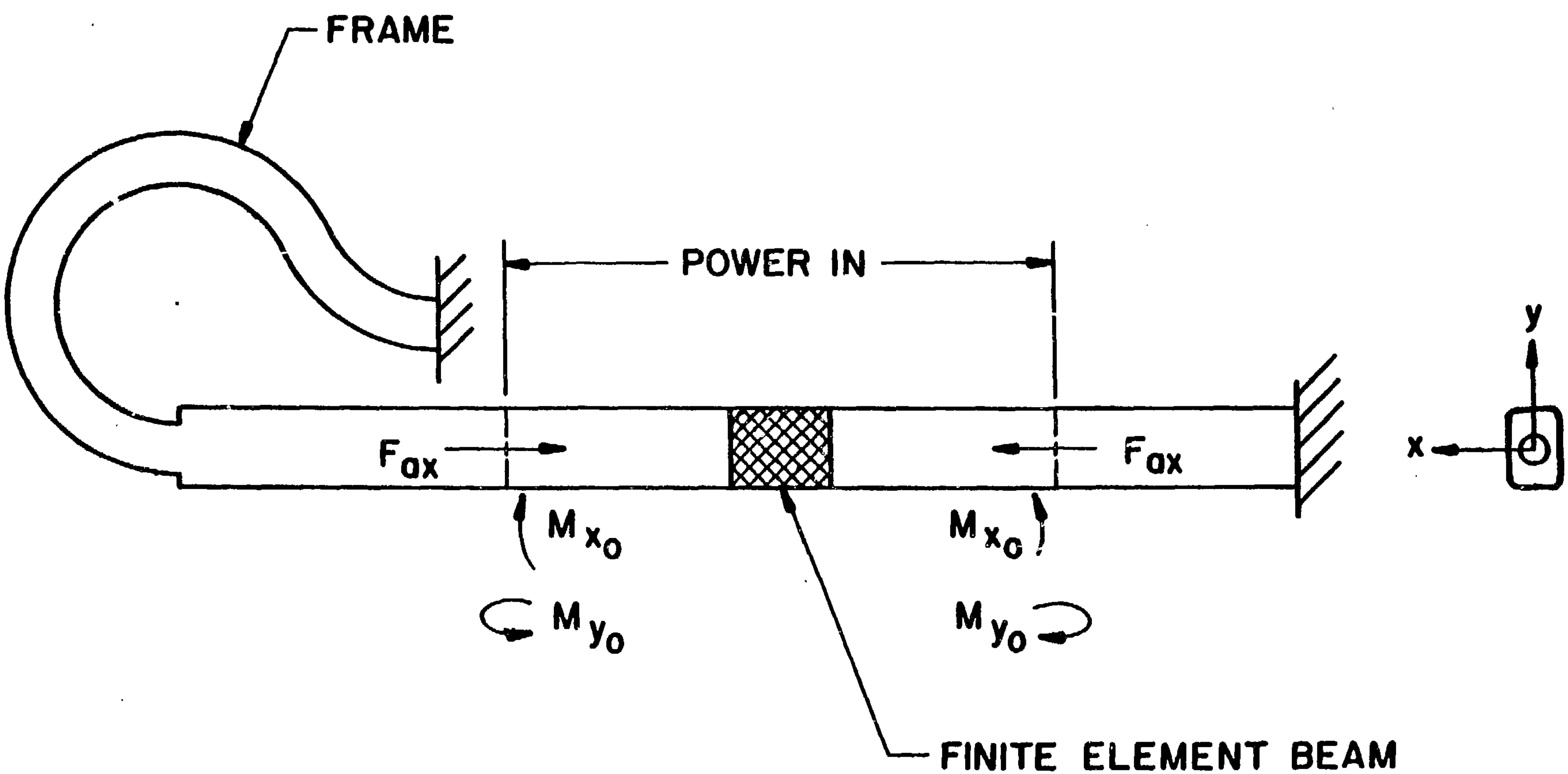

FIG. 5

a

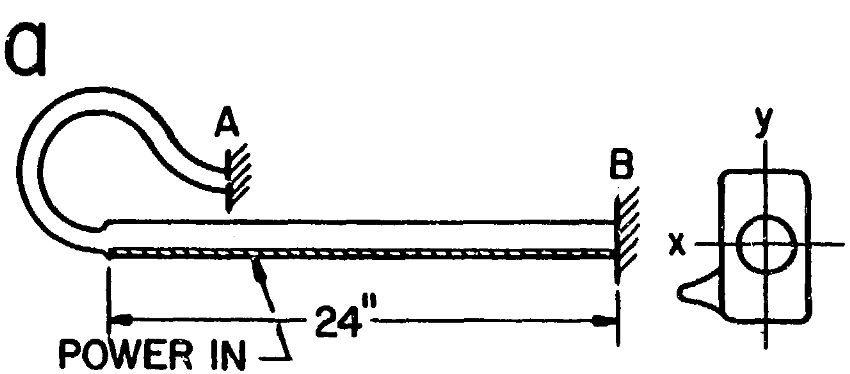

	at A	at B
M_y, lb-in	45	38
M_x, lb-in	124	178
F_{ax}, lb.	31	37
S_{max}, psi	+4600	−14100

b

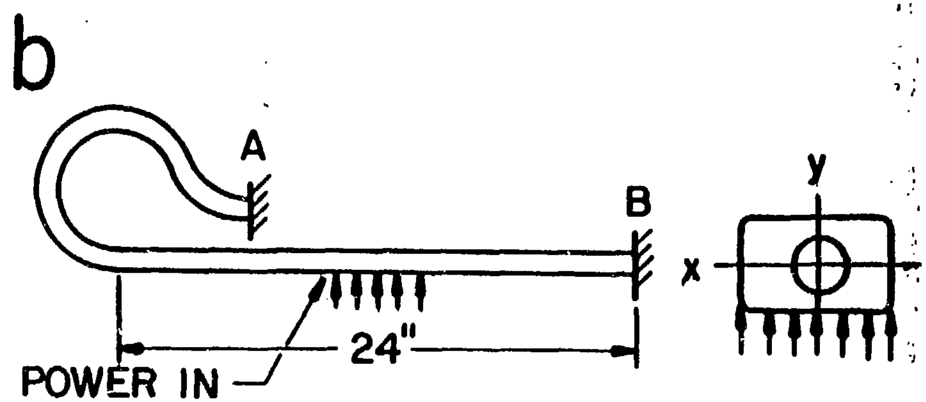

	at A	at B
M_y, lb-in	0	0
M_x, lb-in	90	178
F_{ax}, lb.	43	11
S_{max}, psi	+1600	+6830

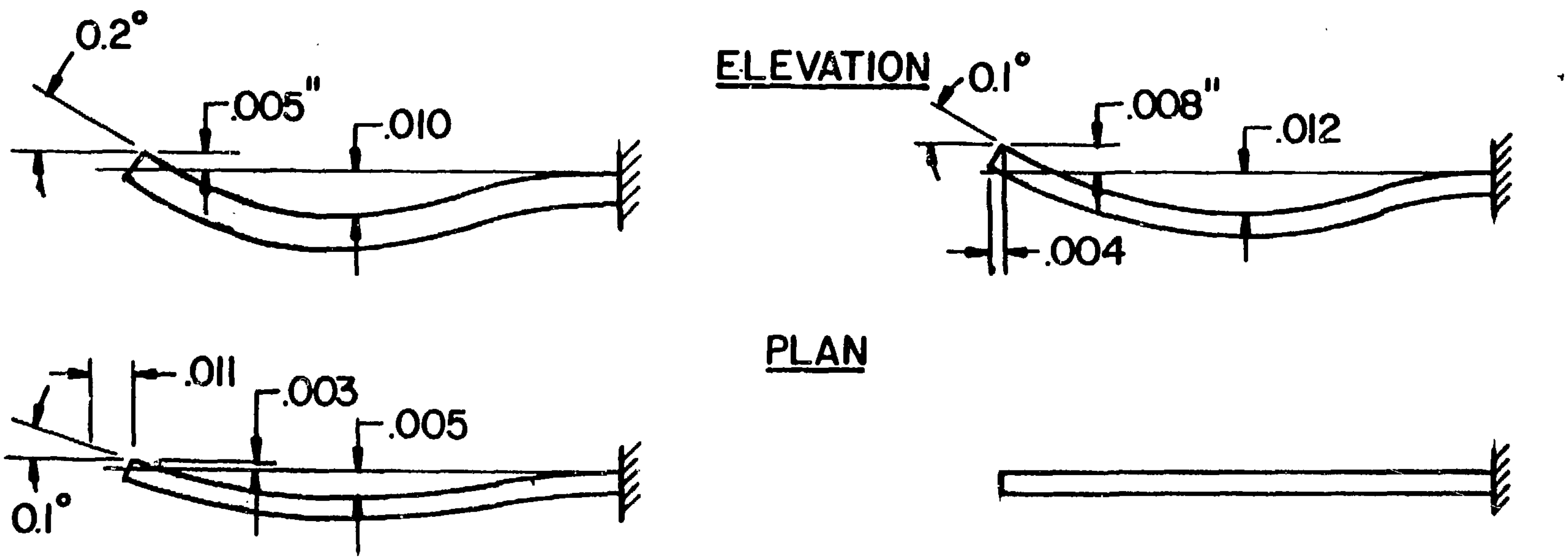

FIG. 6